Electronic Supplementary Material (ESI) for Dalton Transactions.
This journal is © The Royal Society of Chemistry 2021
Please do not adjust margins

Supplementary Information

1. Analyses of the XAFS spectra

A Si(111) crystal was used to monochromatise the synchrotron radiation, and the transmission mode was applied to measure the Pt L_{III} edge absorption spectra. Pt foil (11564 eV) was used for energy calibrations.[S1] Spline approximation of the atomic absorption background of the raw spectra was used to extract the EXAFS signal, which was performed using the ATHENA software package (version 0.8.056).[S2] The k^3-weighted signals were then windowed using the Hann function. Data fitting was performed with version 0.8.012 of the ARTHEMIS software package.[S2] The theoretical phases and amplitudes for the Pt samples were calculated with FEFF6 and based on the structures of $[Pt(NO_3)_6]^{2-}$, $[Pt_2(\mu\text{-}OH)_2(NO_3)_6]^{2-}$, $[Pt_4(\mu_3\text{-}OH)_2(\mu_2\text{-}OH)_4(NO_3)_{10}]$, and $[Pt_6(\mu_3\text{-}OH)_4(\mu_2\text{-}OH)_6(NO_3)_{12}]^{2+}$.[S3,S4] The coordination number of Pt^{4+} was fixed at 6, based on the reported crystal structures. The amplitude-reduction factor was determined by fitting the spectra of the known Pt(IV) complex ($[PtCl_6]^{2-}$) in the 2 M HCl solution.[S5–S7] The obtained value (0.9) was applied in the data fits for all samples. Single scatterings for the Pt–O, Pt–Pt, and Pt–Cl paths and multiple scatterings for a colinear Pt–O–Pt–O path were included in theoretical fittings of the EXAFS and the corresponding Fourier-transformed spectra. The standard deviations were determined with an F test (95% confidence),[S8] and the fitting quality was checked using the R factor defined as follows: $R = \{\sum([Re_{fit}]^2 + [Im_{fit}]^2) / \sum([Re_{obs}]^2 + [Im_{obs}]^2)$, where Re and Im denote the real and imaginary parts of the EXAFS, respectively.

2. Nitrate adsorption tests

Nitric acid solutions (3.0 mL) were mixed with IRC748 resin (0.100 g) in 15-mL plastic tubes. The mixtures were shaken with a high-speed mixer (CM-1000, Tokyo Rikakikai Co.) at 1,800 rpm for 1 h at 25 ± 2 °C. After subsequent centrifugation of the mixtures, the nitrate concentrations in the aqueous solutions were determined by analysing the nitrate absorption band (201 nm) using UV-Vis spectroscopy (UV-2700, Shimadzu). The amounts of NO_3^- adsorbed per 1 g of resin were calculated from the mass balances of NO_3^- in the aqueous solutions. The amounts of NO_3^- adsorbed were verified as shown in Figure S10. Since the initial state of IRC748 is electrically neutral, its adsorption of nitrate ions indicates that its functional groups are protonated and subsequently paired with the nitrate anions.

3. FT-IR spectrometry

Samples of the ion-exchange resins containing metal ions were powdered and their FT-IR spectra were measured using the attenuated total reflection method with a Perkin Elmer Spectrum 100 instrument. Data were collected at wavenumbers of 600–4000 cm^{-1} with a resolution of 4 cm^{-1}. Data collection was repeated 15 times and the datasets were then merged.

Figures

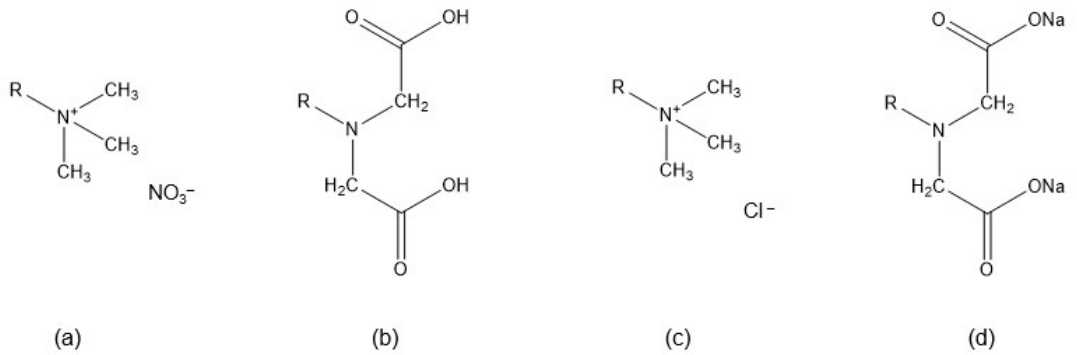

Figure S1. Structural formulae of the ion-exchange resins, where R indicates the base material: (a) IRA900-NO_3^- (R = styrene-divinylbenzene copolymer), (b) IRC748-H^+ (R = polystyrene), (c) IRA900 (R = styrene-divinylbenzene copolymer), and (d) IRC748 (R = polystyrene).

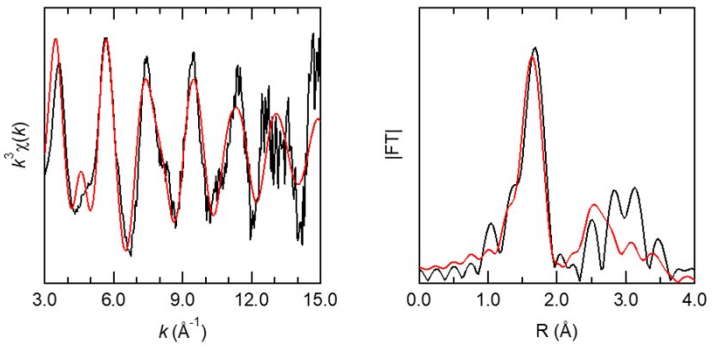

Figure S2. Pt L_{III} edge k^3-weighted extended X-ray absorption fine structure (EXAFS) spectra (left) and the corresponding Fourier-transform (FT) spectra (right) of Pt in PS1 (solutions PS1–PS6 are defined in Table 1). Experimental data (black line) and theoretical data based on the structure of $[Pt(NO_3)_6]^{2-}$ (red line) are shown. The phase shifts are not corrected. The theoretical fitting was calculated from the molecular structure of $[Pt(NO_3)_6]^{2-}$ and includes single scattering of the 6-fold Pt–O (2.01 Å), 6-fold Pt–N (2.94 Å), and 6-fold Pt–O paths (3.06 Å).[S3] However, the theoretical peaks for the coordinated NO_3^- fail to accurately represent the experimental data in the region between 2.0 and 4.0 Å.

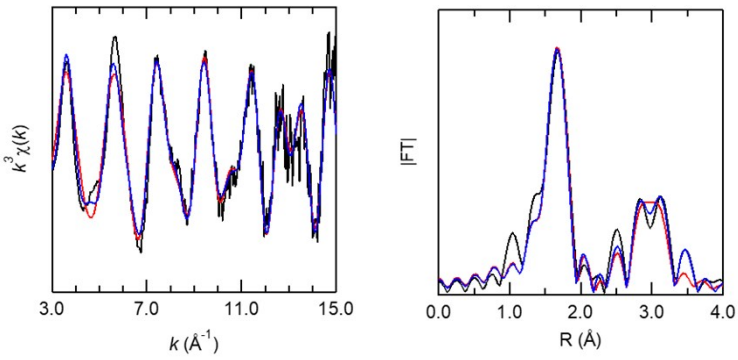

Figure S3. Pt L_{III} edge k^3-weighted EXAFS spectra (left) and the corresponding FT spectra (right) of Pt (3.0 g/L) in PS1. Experimental data (black line) and theoretical data of two-shell fitting (red line), and of three-shell fitting (blue line) are shown. The phase shifts are not corrected.

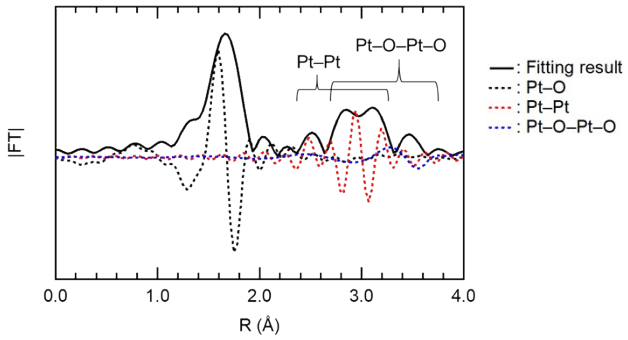

Figure S4. Theoretical fitting of the Pt L_{III} edge k^3-weighted EXAFS FT spectra of Pt (3.0 g/L) in PS1 and its imaginary components of the Pt–O, Pt–Pt, and Pt–O–Pt–O paths. The Pt–Pt correlation roughly profiled the three peaks in the region of 2.4–3.3 Å. The Pt–O–Pt–O correlation represents a peak at 3.5 Å, and additionally, the presence of multiple scattering affected the peak splitting at approx. 3.0 Å.

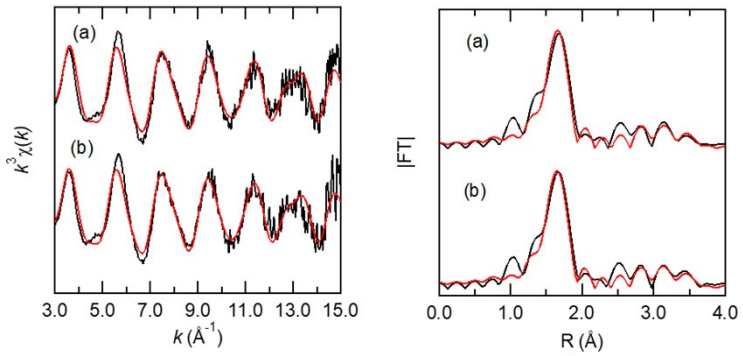

Figure S5. Pt L_{III} edge k^3-weighted EXAFS spectra (left) and the corresponding FT spectra (right) of Pt (3.2 g/L) in PS5 after (a) ageing for 5 d and (b) ageing for 28 d at 25 ± 2 °C. The spectra labelled (b) are the same as those shown in Figure 2(e). Experimental data (black line) and theoretical data (red line) are shown. The phase shifts are not corrected.

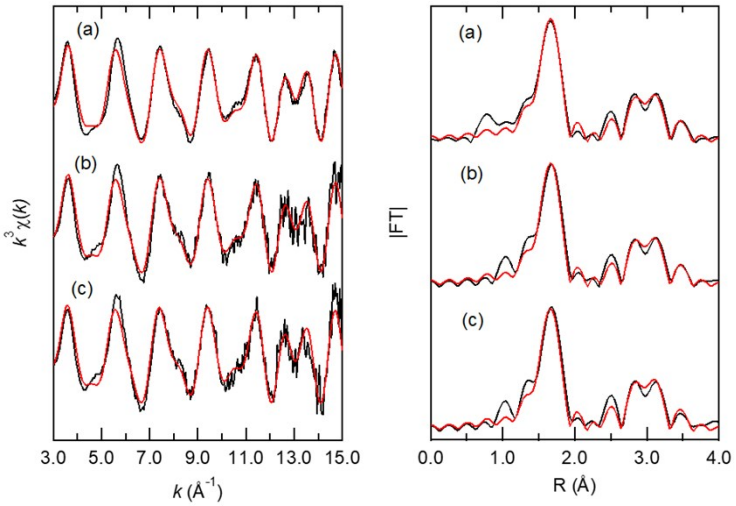

Figure S6. Pt L_{III} edge k^3-weighted EXAFS spectra (left) and the corresponding FT spectra (right) of PS1 after ageing for (a) 12, (b) 28, and (c) 200 d. The spectra labelled (b) are the same as those shown in Figure 2(a). Experimental data (black line) and theoretical data (red line) are shown. The phase shifts are not corrected.

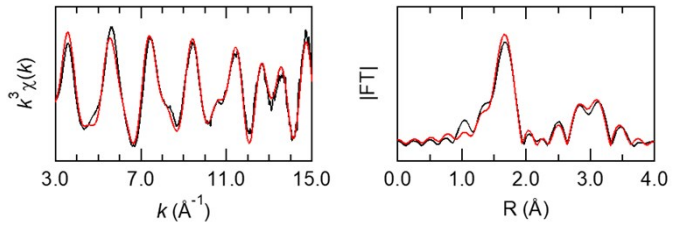

Figure S7. Pt L_{III} edge k^3-weighted EXAFS spectra (left) and the corresponding FT spectra (right) of IRC748-H^+ in the presence of 9.0 mg-Pt/g. Experimental data (black line) and theoretical data (red line) are shown. The phase shifts are not corrected.

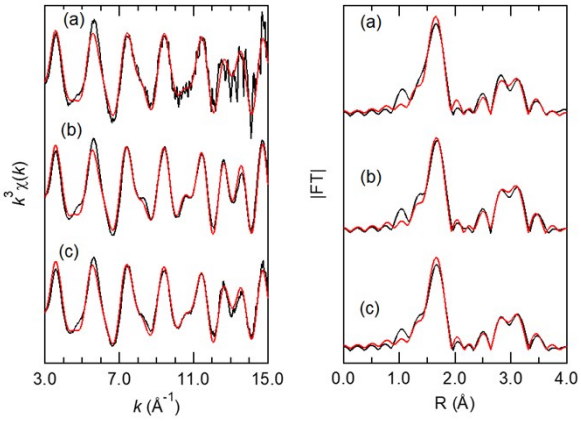

Figure S8. Pt L_{III} edge k^3-weighted EXAFS spectra (left) and the corresponding FT spectra (right) of Pt in the aqueous solution and adsorbed onto the ion-exchange resins in 5 M HNO_3: (a) 5 M HNO_3 solution diluted from PS1 (1.0 g-Pt/L); (b) IRA900-NO_3^- with 36 mg-Pt/g; and (c) IRC748-H^+ with 6.7 mg-Pt/g. Experimental data (black line) and theoretical data (red line) are shown. The phase shifts are not corrected.

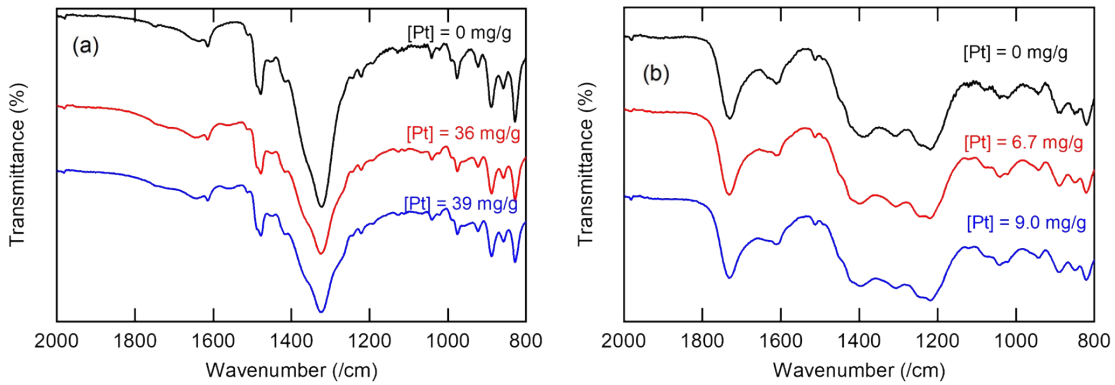

Figure S9. FT-IR spectra of the (a) IRA900-NO_3^- and (b) IRC748-H^+ resins upon the adsorption of Pt(IV). The aqueous solutions that the resins were exposed to are as follows: 5 M HNO_3 solution (black line); 5 M HNO_3 solution containing 1.0 g-Pt/L (red line); and 10 M HNO_3 solution containing 1.1 g-Pt/L (blue line). The prepared Pt(IV) nitrate solutions were dilutions of PS1. Weight of ion-exchange resin: 0.100 g; Aq. volume: 3.0 mL; and shaking time: 72 h.

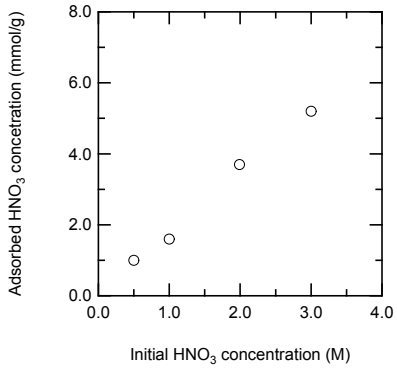

Figure S10. Nitrate concentrations adsorbed onto IRC748. Weight of IRC748: 0.100 g; Aq. volume: 3.0 mL; and shaking time: 1 h.

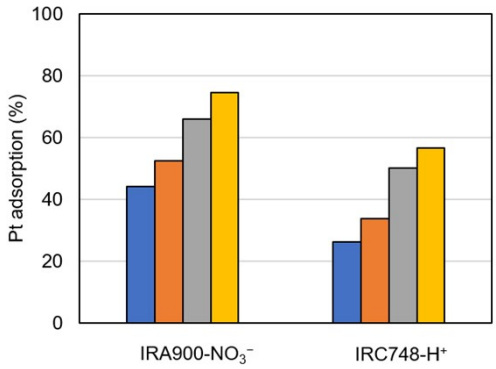

Figure S11. Percentages of Pt(IV) adsorbed by IRA900-NO_3^- and IRC748-H^+ in a 10 M HNO_3 solution. The aqueous solutions were prepared by the dilution of PS4 (0.46 g-Pt/L, blue), PS3 (0.90 g-Pt/L, orange), PS2 (1.5 g-Pt/L, grey), and PS1 (3.0 g-Pt/L, yellow). [Pt]: 50 mg/L; weight of ion-exchange resin: 0.100 g; Aq. volume: 3.0 mL; and shaking time: 72 h.

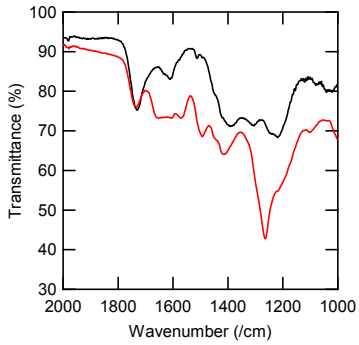

Figure S12. FT-IR spectra of IRC748-H^+-adsorbed Pd(II). The resin was exposed to a 5 M HNO_3 solution (black line) and a 5 M HNO_3 solution containing 0.1 M Pd(II) (red line). The band corresponding to the –COOH moiety at 1730 cm^{-1} shifted to a lower wavenumber (1648 cm^{-1}) upon Pd(II) adsorption.

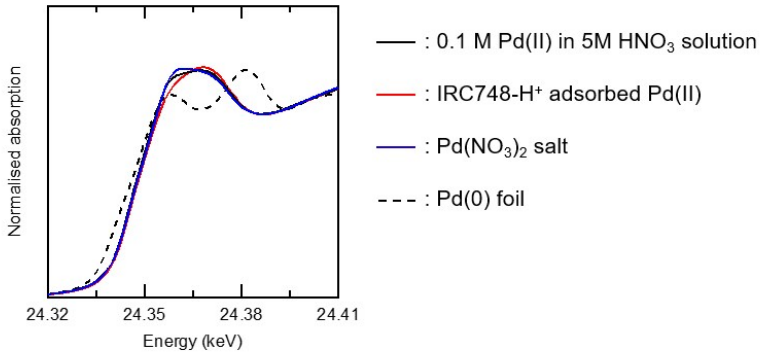

Figure S13. Pd K edge X-ray absorption near edge structure (XANES) spectra of a 5.0 M HNO_3 solution (black line), IRC748-H^+ (red line), $Pd(NO_3)_2$ (blue line), and Pd foil (dotted line).

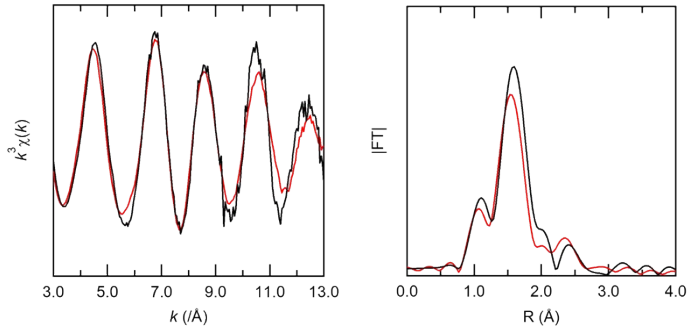

Figure S14. Pd K edge k^3-weighted EXAFS spectra (left) and the corresponding FT spectra (right) of Pd(II) in a 5.0 M HNO_3 solution (black line) and adsorbed onto IRC748-H^+ (red line). The phase shifts are not corrected.

Table S3. Pt L_{III} edge EXAFS structural parameters for the Pt(IV) complexes adsorbed on IRC748-H^+ in 10 M HNO_3

Sample	Pt conc.	Path	*N*	R (Å)	σ^2 (Å^2)[a]	S_0^2 [b]	ΔE	R factor

Table S1. Pt L_{III} edge EXAFS structural parameters for the Pt(IV) complexes in PS5 after ageing for 5 d

Pt conc.	Ageing time	Path	*N*	R (Å)	σ^2 (Å^2)[a]	ΔE (eV)[b]	R factor
3.2 g/L	5 days	Pt–O	6.0 [c]	2.005(4)	0.0025 [c]	13.5(8)	0.0666
		Pt–Pt	1.0(4)	3.09(1)	0.0033 [c]		
		Pt–O(MS)	6.0 [c]	4.031(8)	0.0025 [c]		

[a]Debye–Waller factor. [b]Energy-shift parameter. [c]Fixed parameter. MS = multiple scatterings. Amplitude-reduction factors were fixed as 0.9. Estimated errors are given in parentheses. *k*-range for the Fourier transformation: 3.0–15.0 Å^{-1}; curve-fitting R-range: 1.0–4.0 Å.

Tables

Table S2. Pt L_{III} edge EXAFS structural parameters for the Pt(IV) complexes in PS1 after ageing for 12 and 200 d

Pt conc.	Ageing time	Path	*N*	R (Å)	σ^2 (Å^2)[a]	ΔE (eV)[b]	R factor
3.0 g/L	12 days	Pt–O	6.0 [c]	2.009(2)	0.0025 [c]	13.7(4)	0.0199
		Pt–Pt	2.6(1)	3.082(3)	0.0033 [c]		
		Pt–O(MS)	6.0 [c]	4.040(4)	0.0025 [c]		
3.0 g/L	200 days	Pt–O	6.0 [c]	2.010(4)	0.0029 [c]	13.2(6)	0.0390
		Pt–Pt	2.9(3)	3.083(4)	0.0032 [c]		
		Pt–O(MS)	6.0 [c]	4.042(8)	0.0029 [c]		

[a]Debye–Waller factor. [b]Energy-shift parameter. [c]Fixed parameter. Amplitude-reduction factors were fixed as 0.9. Estimated errors are given in parentheses. *k*-range for the Fourier transformation: 3.0–15.0 Å^{-1}; curve-fitting R-range: 1.0–4.0 Å.

							(eV)[c]	
IRC748-H^+ [d]	9.0 mg/g	Pt–O	6.0 [e]	2.015(3)	0.0029 [e]	0.9 [e]	13.5(5)	0.0267
		Pt–Pt	2.5(3)	3.077(4)	0.0032 [e]			
		Pt–O(MS)	6.0 [e]	4.051(6)	0.0029 [e]			

[a]Debye–Waller factor. [b]Amplitude-reduction factor. [c]Energy-shift parameter. [d]Sample was prepared using PS6. [e]Fixed parameter. Estimated errors are given in parentheses. *k*-range for the Fourier transformation: 3.0–15.0 $Å^{-1}$; curve-fitting R-range: 1.0–4.0 Å.

Table S4. Pt L_{III} edge EXAFS structural parameters for the Pt(IV) complexes in the feed solution and adsorbed on the ion-exchange resins in 5 M HNO_3

Sample	Pt conc.	Path	*N*	R (Å)	σ^2 ($Å^2$)[a]	S_0^2 [b]	ΔE (eV)[c]	R factor
Aqueous solution[d]	1.0 g/L	Pt–O	6.0 [e]	2.002(3)	0.0025 [e]	0.9 [e]	12.5(7)	0.0464
		Pt–Pt	2.5(3)	3.076(6)	0.0033 [e]			
		Pt–O(MS)	6.0 [e]	4.027(6)	0.0025 [e]			
IRA900-NO_3^-	36 mg/g	Pt–O	6.0 [e]	2.016(3)	0.0028(3)	0.9 [e]	13.3(6)	0.0287
		Pt–Pt	2.9(3)	3.078(3)	0.0029(3)			
		Pt–O(MS)	6.0 [e]	4.054(6)	0.0028(3)			
IRC748-H^+	3.4 mg/g	Pt–O	6.0 [e]	2.014(3)	0.0029 [e]	0.9 [e]	13.3(5)	0.0268
		Pt–Pt	2.3(3)	3.078(5)	0.0032 [e]			
		Pt–O(MS)	6.0 [e]	4.049(6)	0.0029 [e]			

[a]Debye–Waller factor. [b]Amplitude-reduction factor. [c]Energy-shift parameter. [d]Solution was prepared by the dilution of PS1. [e]Fixed parameter. Estimated errors are given in parentheses. *k*-range for the Fourier transformation: 3.0–15.0 $Å^{-1}$; curve-fitting R-range: 1.0–4.0 Å.

References

[S1] J. A. Bearden and A. F. Burr, *Rev. Mod. Phys.*, 1967, **39**, 125.

[S2] B. Ravel and M. Newville, *J. Synchrotron Rad.*, 2005, **12**, 537.

[S3] D. Vasilchenko, S. Tkachev, I. Baidina and S. Korenev, *Inorg. Chem.*, 2013, **52**, 10532.

[S4] D. B. Vasilchenko, S. V. Tkachev, and A. C. Tsipis, *Eur. J. Inorg. Chem.*, 2018, **2018**, 627.

[S5] K. C. Sole, in Solvent Extraction and Liquid Membranes, eds. M. Aguilar and J. L. Cortina, CRC Press, Boca Raton, FL, 1st Ed., 2008, Chap. 5, 141.

[S6] W. A. Spieker, J. Liu, J. T. Miller, A. J. Kropf and J. R. Regalbuto, *Appl. Catal. A*, 2002, **232**, 219.

[S7] J. Kramer and K. R. Koch, *Inorg. Chem.*, 2006, **45**, 7843.

[S8] K. V. Klementev, *J. Synchrotron Rad.*, 2001, **8**, 270.